Keratinocyte-intrinsic MHCII expression controls microbiota-induced Th1 cell responses

Samira Tamoutounour[a,1,2], Seong-Ji Han[a,1], Julie Deckers[b,c], Michael G. Constantinides[a], Charlotte Hurabielle[a,d,3], Oliver J. Harrison[a], Nicolas Bouladoux[a,e], Jonathan L. Linehan[a,4], Verena M. Link[a], Ivan Vujkovic-Cvijin[a], Paula Juliana Perez-Chaparro[e], Stephan P. Rosshart[f,5], Barbara Rehermann[f], Vanja Lazarevic[g], and Yasmine Belkaid[a,e,6]

[a]Metaorganism Immunity Section, Laboratory of Immune System Biology, National Institute of Allergy and Infectious Diseases, National Institutes of Health, Bethesda, MD 20892; [b]Immunoregulation Unit, Vlaams Instituut voor Biotechnologie Center for Inflammation Research, 9052 Ghent, Belgium; [c]Department of Internal Medicine, Ghent University, 9000 Ghent, Belgium; [d]Inserm U976, Hôpital Saint Louis, Université Paris Diderot, 75010 Paris, France; [e]National Institute of Allergy and Infectious Diseases Microbiome Program, National Institutes of Health, Bethesda, MD 20892; [f]Immunology Section, Diseases Branch, National Institute of Diabetes and Digestive and Kidney Diseases, National Institutes of Health, Bethesda, MD 20892; and [g]Experimental Immunology Branch, National Cancer Institute, National Institutes of Health, Bethesda, MD 20892

The cross-talk between the microbiota and the immune system plays a fundamental role in the control of host physiology. However, the tissue-specific factors controlling this dialogue remain poorly understood. Here we demonstrate that T cell responses to commensal colonization are associated with the development of organized cellular clusters within the skin epithelium. These organized lymphocyte clusters are surrounded by keratinocytes expressing a discrete program associated with antigen presentation and antimicrobial defense. Notably, IL-22–mediated keratinocyte-intrinsic MHC class II expression was required for the selective accumulation of commensal-induced IFN-γ, but not IL-17A–producing CD4+ T cells within the skin. Taking these data together, this work uncovers an unexpected role for MHC class II expression by keratinocytes in the control of homeostatic type 1 responses to the microbiota. Our findings have important implications for the understanding of the tissue-specific rules governing the dialogue between a host and its microbiota.

microbiota | skin | keratinocyte | antigen presentation | Th1

The microbiota play a fundamental role in the induction and quality of local immune responses (1). A large fraction of this response is directed at the microbiota itself (1, 2). Notably, adaptive recognition of the microbiota controls several aspects of tissue physiology, including antimicrobial defense and tissue repair (1–4). As such, identification of the factors controlling the quality and function of commensal-induced T cells has important implications for our understanding of host immunity and tissue pathologies.

Commensal-specific T cells exert their local function via the release of defined cytokines, such as interleukin (IL)-17A and IL-22, the production of which is tightly regulated by local cues (1). Indeed, adaptive immunity to commensal microbes relies on a highly controlled sequence of events, including functional licensing by tissue-specific factors or mechanisms. Epithelial cells, as the first-line in the host microbiota dialogue, play a critical role in these processes. For example, within the gastrointestinal tract, segmented filamentous bacteria promote the production of serum amyloid A (SAA) by intestinal epithelial cells. SAA in turn licenses IL-17A production by segmented filamentous bacteria-specific CD4+ T cells (5). Furthermore, in the gut, epithelial cell responses to the microbiota—particularly the production of IL-18, IL-25, IL-33, and thymic stromal lymphopoietin—have been shown to control both the frequency and function of innate lymphoid cells (ILCs) (6). Evidence also supports the idea that commensal-induced cues are tissue-specific. For example, within the skin, the ability of the microbiota to promote local production of IL-1α and IL-23 licenses cutaneous T cells to release IL-17A (7, 8). However, much remains to be learned about how defined microenvironments can shape the host–microbiota dialogue. More particularly, the extent to which epithelial cells from distinct compartments respond to commensals in a way that supports defined classes of adaptive immunity remains poorly understood.

Here we found that the ability of commensal-specific Th1 cells to accumulate within the skin was associated with the physical organization of T cells within epidermal lymphocyte clusters. Within these clusters, interferon-γ (IFN-γ) production by CD4+ T cells was controlled by major histocompatibility complex class II (MHCII)-expressing keratinocytes. Taken together, our work uncovers a tissue checkpoint involved in the discrete control

Significance

The cross-talk between the microbiota and the immune system plays a fundamental role in the control of host physiology. However, the tissue-specific factors controlling this dialogue remain poorly understood. Here we demonstrate that T cell responses to commensal colonization are associated with the development of organized cellular clusters within the skin epithelium. Keratinocyte-intrinsic MHC class II expression was required for the selective accumulation of commensal-induced IFN-γ–producing CD4+ T cells within the skin. This work uncovers an unexpected role for MHC class II expression by keratinocytes in the control of homeostatic type 1 responses to the microbiota. Our findings have important implications for the understanding of the tissue-specific rules governing the dialogue between a host and its microbiota.

IMMUNOLOGY AND INFLAMMATION

Fig. 1. *S. epidermidis* induces MHCII[+] keratinocytes and lymphocyte clusters in the epidermis. (*A*) Representative confocal microscopy image of a projection on the *z* axis of an *Il17a*^Cre^*Rosa26*^YFP^ (IL-17A^YFP^) mouse epidermis stained for CD8α, CD4, and CD49f at day 14 postassociation with *S. epidermidis*. HF: Hair follicle. (Scale bars, 30 μm.) (*B*) Representative confocal microscopy image of a projection on the *z* axis of a T-bet^ZsGreen^ mouse epidermis stained for CD8α, CD4, and CD49f at day 14 postassociation with *S. epidermidis.* HF: Hair follicle. (Scale bars, 20 μm.) (*C*) Representative confocal microscopy image of C57BL/6 mouse epidermis stained for CD8α, CD4, MHCII, and CD49f at day 14 postassociation with *S. epidermidis*. MHCII^{+}CD49f^{+} keratinocytes result from colocalization between MHCII^{+} and CD49f^{+} cells. (Scale bars, 100 μm or 50 μm.) Dotted orange lines show the delineation of the areas containing CD49f^{+}MHCII^{+} keratinocytes. (*D*) Flow cytometric analysis of MHCII expression by epidermal CD49f^{+} keratinocytes from unassociated control mice or mice at day 14 postassociation with *S. epidermidis*. (*E*) Frequencies of EdU incorporation by MHCII[+] keratinocytes and MHCII[−] keratinocytes at 14 d after *S. epidermidis* association. (*F*) Frequencies of MHCII[+] keratinocyte populations by indicated cellular phenotype. (*G*) Schematic illustrating the anatomical localization of distinct keratinocyte populations. Graph represents the frequencies of MHCII expression by distinct keratinocyte populations. (*H–K*) Frequencies of epidermal MHCII[+] keratinocytes in control (Ctrl) unassociated mice or in mice associated with different strains (LM061, LM087, NIH05001) of *S. epidermidis* (*H*), in *S. epidermidis* (LM087)-associated germ-free mice (*I*), and in mice associated with *S. aureus* (*J*) or *C. albicans* (*K*) at day 14 postassociation. (*L*) Frequencies of MHCII[+] keratinocytes in C57BL/6 SPF (B6 SPF) mice, C57BL/6 GF mice conventionalized with wild mouse microbiota (B6 Conv) and in wild mice (Wild). Student's *t* test was used to measure significance. *$P < 0.05$, **$P < 0.01$, and ***$P < 0.001$. Data are presented as mean only or mean ± SEM. Data are representative of 2 to 4 independent experiments.

of commensal-specific T cells, and an unexpected role for MHCII expression by keratinocytes in the licensing of homeostatic tissue-specific immunity.

Results

Commensal-Induced T Cells Accumulate in Epidermal Clusters Surrounded by Activated Keratinocytes. We previously showed that colonization with defined skin commensals resulted in the accumulation of commensal-specific CD4^{+} and CD8^{+} T cells within the skin, a process uncoupled from inflammation (3, 7, 9). Notably, skin association with live *Staphylococcus epidermidis* induced the accumulation of commensal-reactive Th1 and Th17 (*SI Appendix*, Fig. S1*A*) (9) as well as Tc1 and Tc17 cell subsets (3, 9). In a similar manner to tissue-resident memory CD8^{+} T cells induced by viral infection (10), long-lived *S. epidermidis*-specific CD8^{+} T cells have a tropism for the epidermis (4, 9), as shown by their colocalization with epidermal CD49f^{+} keratinocytes (Fig. 1 *A* and *B*). Strikingly, we found that Th17 and Th1 cells induced by *S. epidermidis* colonization (visualized as IL-17A[YFP]- or T-bet[ZsGreen]-expressing CD4^{+} T cells, respectively) colocalized with CD8^{+} T cells in discrete clusters within the epidermal compartment (Fig. 1 *A* and *B*). Dermal and hair follicle-associated lymphocyte clusters have been previously identified in the context of inflammatory settings. Notably, lymphocyte clusters following infection can promote cutaneous responses by retaining lymphocytes within the skin or the urogenital tract (11–13). However, the function and properties of epidermal lymphocyte clusters, and more particularly those associated with commensal-induced responses, remain unclear. The defined spatial organization of lymphocytes in response to *S. epidermidis* association supported the idea that commensal-induced T cells may establish privileged interactions with neighboring keratinocytes. In support of this, keratinocytes surrounding T cell epidermal clusters expressed high levels of MHCII (Fig. 1*C*). Increased frequencies of MHCII expression by CD49f^{+} keratinocytes following neocolonization was confirmed by flow cytometry (Fig. 1*D*). CD49f^{+} keratinocytes expressing MHCII also showed higher frequencies of 5-ethynyl-2′-deoxyuridine (EdU) incorporation than MHCII^{−}CD49f^{+} keratinocytes, highlighting their higher rates of proliferation (Fig. 1*E*). This supported the idea that keratinocytes in contact with commensal-induced T cells were in an activated state. A short period of EdU incorporation revealed that skin T cells also showed a higher rate of proliferation 2 weeks postassociation (*SI Appendix*, Fig. S1*B*).

Keratinocytes can be classified into distinct subsets according to their localization and association with the hair follicle, based on their relative expression of CD49f, Sca-1, CD34, and EpCAM (*SI Appendix*, Fig. S1*C*) (14). Following *S. epidermidis* association, interfollicular, infundibular, and isthmic keratinocytes expressed MHCII at a similar frequency, although MHCII[+] interfollicular keratinocytes were numerically dominant (Fig. 1 *F* and *G*). Interfollicular keratinocytes are derived from basal keratinocytes, whereas infundibular and isthmic keratinocytes are derived from hair follicle stem cells (15), thus MHCII expression by keratinocytes may not be restricted to a specific keratinocyte lineage. Consistently, MHCII[+] keratinocytes were found in the interfollicular epidermis and in the isthmic and infundibular areas of the hair follicle (Fig. 1 *A–C*). In contrast, basal bulge and suprabasal bulge keratinocytes showed significantly lower MHCII expression (Fig. 1*G*), in agreement with the known ability of these subsets to evade immune surveillance in order to maintain hair follicle homeostasis (16). Frequencies of MHCII^{+} keratinocytes and numbers of epidermal CD4^{+} T cells decreased over time but remained higher than in unassociated control mice, while epidermal resident memory CD8^{+} T cell numbers remained unchanged over time (*SI Appendix*, Fig. S1*D*). Previous work also showed that under steady-

state conditions, a small fraction of human keratinocytes expressed HLA-DR, a human MHCII molecule (17).

We next assessed if this response was restricted to a defined microbial interaction. We previously demonstrated that while all *S. epidermidis* strains tested induced CD4^{+} T cell accumulation, only a defined clade could induce CD8^{+} T cell responses (3). Expression of MHCII by keratinocytes was conserved across *S. epidermidis* strains regardless of their ability to induce CD8^{+} T cells (Fig. 1*H*). Up-regulation of MHCII by keratinocytes was also observed in germ-free (GF) mice monoassociated with *S. epidermidis,* demonstrating that this response can be mediated by the addition of a single commensal (Fig. 1*I*). Activation of keratinocytes postassociation was also observed at other skin sites (e.g., back skin) (*SI Appendix*, Fig. S1*E*) and conserved following colonization with other members of the skin microbiota, such as *Staphylococcus aureus* and *Candida albicans* (Fig. 1 *J* and *K*). Thus, T cell responses to a new skin commensal are associated with the discrete clustering of lymphocytes within the epidermis and their tight association with activated keratinocytes.

We next assessed if the low frequencies of MHCII expression by keratinocytes observed at steady state could be explained by a lack of physiological microbial stimulation. Recent studies showed that wild-caught outbred mice that are exposed to physiological microbial partners exhibit higher immune fitness (18, 19). Indeed, while granulocyte and monocyte frequencies were unaffected, we found that wild mice (Wild) and C57BL/6 germ-free mice conventionalized with wild mouse microbiota (B6 Conv) (20) showed higher frequencies of MHCII[+] keratinocytes than C57BL/6 SPF (B6 SPF) mice at steady state (Fig. 1*L* and *SI Appendix*, Fig. S1*F*). Thus, MHCII expression by keratinocytes is a physiological feature of the skin that can be promoted by homeostatic encounter with relevant commensal microbes.

Cluster-Associated Keratinocytes Express a Transcriptional Profile Associated with T Cell Homing/Retention and Antigen Presentation. To more comprehensively assess keratinocyte responses to microbial colonization, we performed RNA sequencing (RNA-seq) of highly purified CD49f^{+}Sca-1^{+}MHCII^{+} keratinocytes (MHCII^{+} as a surrogate for cluster-associated keratinocytes, *S. epi* MHCII^{+}), CD49f^{+}Sca-1^{+}MHCII^{−} keratinocytes (*S. epi* MHCII^{−}) isolated from the skin of mice previously associated with *S. epidermidis*, and CD49f^{+}Sca-1^{+}MHCII^{−} keratinocytes isolated from unassociated control mice (Ctrl MHCII^{−}) (*SI Appendix*, Fig. S2*A*). Principal component analysis (PCA) and variance analysis showed a high similarity between CD49f^{+}Sca-1^{+}MHCII^{−} keratinocytes from *S. epidermidis*-colonized and control mice, supporting the idea that keratinocyte activation in response to commensal association is highly discrete and restricted to sites of interaction with lymphocytes (Fig. 2*A*). On the other hand, CD49f^{+}Sca-1^{+}MHCII^{+} keratinocytes were significantly distinct from CD49f^{+}Sca-1^{+}MHCII^{−} keratinocytes from *S. epidermidis*-associated and control mice ($R^2 = 0.54$, $P = 0.016$) and resembled more interfollicular epidermal basal cells than interfollicular epidermal differentiated cells (Fig. 2*A* and *SI Appendix*, Fig. S2*B*) (21). This was in agreement with our confocal imaging revealing enrichment of MHCII^{+} keratinocytes at the proximity of the basement membrane and the basal layer of the epidermis (*SI Appendix*, Fig. S2*C*). CD49f^{+}Sca-1^{+}MHCII^{+} keratinocytes expressed transcripts for neuropeptides (e.g., *Pyy*, *Nppb*) and antimicrobial peptides (e.g., *Defb6*, *S100a8/9*, *Stfa1*, *Serpinb1a*) (Fig. 2*B*) that have been implicated in barrier defense, keratinocyte differentiation, and orchestration of adaptive and innate lymphocyte responses (9, 22). Furthermore, CD49f^{+}Sca-1^{+}MHCII^{+} keratinocytes expressed elevated levels of chemokines previously shown to be implicated in lymphocyte tropism (Fig. 2*C*). Specifically, MHCII[+] keratinocytes up-regulated *Cxcl16* expression compared to controls, previously shown to be implicated in the retention and clustering of ILCs in the intestine (23) and *Ccl20* and *Cxcl9/10* previously shown to
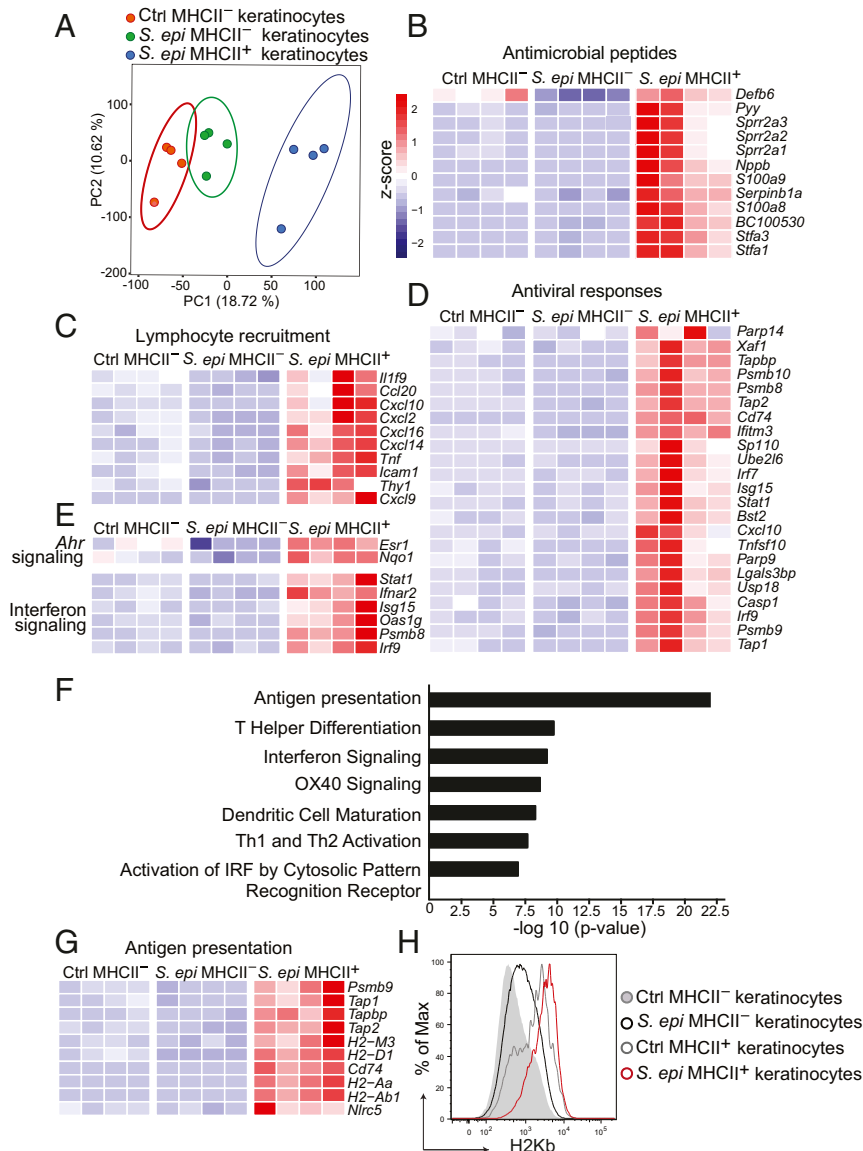
Fig. 2. MHCII⁺ keratinocytes participate in lymphocyte education. (*A–G*) CD49f⁺Sca-1⁺MHCII⁻ keratinocytes from unassociated control (Ctrl MHCII⁻), *S. epidermidis*-associated mice (*S. epi* MHCII⁻) and CD49f⁺Sca-1⁺MHCII⁺ keratinocytes from *S. epidermidis*-associated mice (*S. epi* MHCII⁺) were sorted from CD45⁻CD34⁻CD31⁻ epidermal cell suspension at day 14 postassociation and analyzed by RNA-seq. (*A*) PCA of RNA-seq performed on CD49f⁺Sca-1⁺MHCII⁻ keratinocytes from unassociated control or *S. epidermidis*-associated mice and CD49f⁺Sca-1⁺MHCII⁺ keratinocytes from *S. epidermidis*-associated mice. Ellipses represent 95% confidence intervals of the mean. (*B–E*) Heatmaps showing expression of genes encoding antimicrobial peptides in 4 replicates per condition (*B*), genes associated with lymphocyte recruitment (*C*), antiviral responses (*D*), and Ahr and IFN signaling (*E*). (*F*) IPA of genes up-regulated in CD49f⁺Sca-1⁺MHCII⁺ keratinocytes vs. CD49f⁺Sca-1⁺MHCII⁻ keratinocytes from *S. epidermidis*-associated mice (*G*) Heatmap showing expression of genes implicated in antigen presentation. (*H*) Expression of H2Kb by CD49f⁺Sca-1⁺MHCII⁺ keratinocytes and CD49f⁺Sca-1⁺MHCII⁻ keratinocytes in control mice or day 14 after association with *S. epidermidis*.

support, respectively, the accumulation of IL-17A and IFN-γ producing T cells in the skin (24, 25).

On the other hand, MHCII-expressing keratinocytes did not express transcripts associated with the production of factors know to affect local T cell cytokine production, such as SAAs (*Saa1*, *Saa*2, *Saa*3) or retinoic acid production (*Adh1a1*, *Adh1a2*, *Adh1a3*). They also did not express heightened levels of *Il18* or *Il6* but did display a small increase in *Il1a* transcript levels postassociation (*SI Appendix*, Fig. S2D). Thus, keratinocytes associated with commensal-induced epidermal lymphocyte clusters expressed a gene signature potentially favorable for commensal-specific T cell homing/retention within the epidermis. Of interest, CD49f⁺Sca-1⁺MHCII⁺ keratinocytes also expressed higher levels

of genes implicated in antiviral and IFN responses (Fig. 2 *D* and *E*) and genes implicated in the antioxidant functions of the aryl hydrocarbon receptor (*Ahr*) pathway (26), such as NADPH/ quinone oxidoreductase (*Nqo1*) (Fig. 2*E*). In agreement with enhanced MHCII expression, Ingenuity Pathway Analysis (IPA) of CD49f⁺Sca-1⁺MHCII⁺ keratinocytes' most up-regulated genes showed a significant increase of pathways implicated in antigen processing and presentation (e.g., *Tap1*, *Tap2*, *Cd74*) (Fig. 2 *F* and *G*). CD49f⁺Sca-1⁺MHCII⁺ keratinocytes also showed higher levels of *Nlrc5* transactivator of the major histocompatibility complex class I (MHCI) (16) and classic and nonclassic MHCI genes, including *H2-M3* (Fig. 2*G*), to which *S. epidermidis* CD8⁺ T cells are restricted (3). Furthermore, expression of MHCI

(H2Kb) was also increased in MHCII$^+$ keratinocytes compared to MHCII$^-$ keratinocytes following association with *S. epidermidis* (Fig. 2*H*). Thus, lymphocyte cluster-associated keratinocytes express a broad transcriptional program, including increased antigen processing and presentation pathways.

Commensal-Induced IL-22 Promotes MHCII Expression by Keratinocytes. While keratinocytes associated with commensal-induced epidermal clusters may play a myriad of roles in the control of skin physiology, we focused our attention on their selective and unusual expression of MHCII molecules. This question is of particular interest, as a physiological role for antigen presentation by keratinocytes has not been previously reported in vivo. We first explored the factors responsible for MHCII expression by keratinocytes.

Previous work showed that under inflammatory settings IFN-γ could up-regulate the expression of this molecule by keratinocytes (27). However, in line with the observation that *S. epidermidis* association is noninflammatory (7, 9), MHCII up-regulation by keratinocytes was independent of both type 1 or type 2 IFNs, as well as tumor necrosis factor α (TNF-α) (as shown with *Ifng*$^{-/-}$, *Ifnar*$^{-/-}$, and *Tnfa*$^{-/-}$ mice) (*SI Appendix*, Fig. S3*A*). STAT3 phosphorylation coordinates a broad range of epithelial-mediated responses (28–30). Following *S. epidermidis* colonization, a significant increase in MHCII expression by keratinocytes was detectable by day 7 postcolonization (Fig. 3*A*), while STAT3 phosphorylation in keratinocytes was observed day 5 postcolonization with *S. epidermidis* (Fig. 3*B*). In this context, a cytokine of particular interest is IL-22, which has been previously shown to regulate epithelial cell function in a STAT3-dependent manner (30–32). Indeed, *S. epidermidis*-induced MHCII expression by keratinocytes was abrogated in mice deficient in IL-22 (*Il22*$^{-/-}$) or in WT (wild type) mice treated with anti–IL-22 neutralizing antibody (αIL-22) (Fig. 3 *C* and *D*). On the other hand, no differences were observed in the basal level of MHCII expression between unassociated WT and *Il22*$^{-/-}$ mice (*SI Appendix*, Fig. S3*B*). In contrast, genetic deficiency in additional molecules previously shown to mediate host microbiota interaction [IL-1 α/β, IL-17A, IL-18, IL-23, and Ahr (1)] did not impact the ability of keratinocytes to up-regulate MHCII (Fig. 3*E*).

The cytokine IL-22 can be produced by numerous cell types, including innate and adaptive lymphocytes (33). As early as day 3 postassociation we found that, in the epidermis, the number of γδTCR^{low} cells (and at day 7 for CD8$^+$T cells) expressing IL-22 were significantly increased compared to control mice (Fig. 3 *F* and *G*). A transient increase in IL-22–expressing γδTCR^{low} cells was also observed within the dermis, though this phenomenon was delayed in comparison to that within the epidermis as it began by day 7 postassociation (*SI Appendix*, Fig. S3 *C* and *D*). In addition, both intracellular cytokine staining of IL-22 (Fig. 3 *F* and *G* and *SI Appendix*, Fig. S3 *C* and *D*) and RFP expression in IL-22^{RFP} mice (*SI Appendix*, Fig. S3*E*) demonstrated that epidermal lymphocytes expressed higher frequencies of IL-22 following commensal association, showing a preferential tropism of IL-22 producers to the epidermis. The early IL-22 production by γδTCR^{low} cells following *S. epidermidis* association, as well as their unusual tropism within the epidermis, pointed to a potential role for this cell subset in keratinocyte activation. However, mice deficient in γδTCR cells (*Tcrd*$^{-/-}$) still up-regulated MHCII expression by keratinocytes when compared to WT mice following association (Fig. 3*H*). Furthermore, no differences in MHCII expression by keratinocytes were observed in mice deficient in CD8$^+$ T cells following *S. epidermidis* association (*H2-M3*$^{-/-}$) (3) or in mice in which all mature αβ T cells were deficient in RORγt (*Lck*^{Cre}*Rorc*$^{fl/fl}$), and as such were incapable of producing IL-22 (Fig. 3 *I* and *J* and *SI Appendix*, Fig. S3*F*).

This supported the idea that the cellular origin of IL-22 was either redundant or dependent on ILCs. Numerous ILC subsets have been described at all barrier sites, including the skin (34–36). Following *S. epidermidis* association, the skin contains ILCs (CD90.2$^+$γδTCR$^-$TCRβ$^-$CD4$^-$) expressing high levels of IL-7Rα and CCR6 and low levels of MHCII (*SI Appendix*, Fig. S3 *G* and *H*). Among the ILCs that accumulate after *S. epidermidis* association, $47.7 \pm 6.7\%$ were type 2 ILCs, as shown by GATA-3 expression, with $3.8 \pm 0.8\%$ of ILCs that can be classified as type 3 ILCs expressing RORγt (Fig. 3*K*). Previous work revealed that IL-22 could be produced by both type 3 T-bet$^+$ Nkp46$^+$ILCs and type 3 T-bet$^-$ ILCs (37–39). Following *S. epidermidis* colonization, around 70% of IL-22$^+$ cells were type 3 T-bet$^-$ ILCs (Fig. 3*K*). In the skin, RORγt$^+$ ILCs did not express Nkp46 nor YFP in *Ncr1*^{Cre}*Rosa26*^{YFP} mice, and as such could not be selectively depleted (*SI Appendix*, Fig. S3 *H* and *I*). To assess how, in a simplified model, ILCs may be sufficient to promote keratinocyte activation, we used *Rag2*$^{-/-}$ and *Rag1*$^{-/-}$ mice. In those mice, ILCs are overrepresented (34) and are the only potential source of IL-22 (*SI Appendix*, Fig. S3*J*). We also utilized *Rag2*$^{-/-}$*Il2rg*$^{-/-}$ mice that are devoid of all lymphocytes, including ILCs (40). While *S. epidermidis* was able to induce MHCII expression by keratinocytes in *Rag2*$^{-/-}$ mice, this response was abrogated in *Rag2*$^{-/-}$*Il2rg*$^{-/-}$ mice (Fig. 3*L*). IL-22 neutralization in *Rag1*$^{-/-}$ mice also resulted in reduced frequency of MHCII$^+$ keratinocytes in response to *S. epidermidis* (*SI Appendix*, Fig. S3*K*). ILCs producing IL-22 (IL-22^{tdt+} epidermal lymphocytes) were found in both the epidermis and the dermis postassociation in *Rag2*$^{-/-}$ mice, and could be found in close proximity to keratinocytes expressing MHCII (*SI Appendix*, Fig. S3 *L* and *M*). Thus, under these specific settings, IL-22 production by ILCs was necessary and sufficient for the expression of MHCII by keratinocytes. However, ILCs are overrepresented in *Rag2*$^{-/-}$ and *Rag1*$^{-/-}$ mice and, as such, in WT mice keratinocyte activation is likely to be under the control of redundant cellular sources, including γδ T cells, αβ T cells, and ILCs. Together these results support the idea that lymphocyte-derived IL-22 induced by *S. epidermidis* association promoted the discrete activation of keratinocytes and, more particularly, MHCII expression.

Monocyte-Derived Cells Promote Both Th1 Responses and MHCII Expression by Keratinocytes. While Langerhans cells (LCs) account for 96% of the antigen-presenting cells present in the epidermis, we found that these cells were not necessary for the induction of MHCII expression by keratinocytes (Fig. 4 *A* and *B*). On the other hand, in *Ccr2*$^{-/-}$ mice that are deficient in monocyte-derived cell accumulation within tissue (41), both expression of MHCII by keratinocytes and Th1 cell accumulation (but not Th17) in response to *S. epidermidis* were significantly reduced compared to WT mice (Fig. 4 *C*–*E*). Such defects were not T cell-intrinsic (*SI Appendix*, Fig. S4*A*). However, the production of IL-22 was unchanged in *Ccr2*$^{-/-}$ mice, supporting the idea that monocyte-derived cells are necessary to coordinate both Th1 accumulation and MHCII expression by keratinocytes downstream of IL-22 (*SI Appendix*, Fig. S4*B*). These results also pointed to a potential link between MHCII expression by keratinocytes and the ability of commensal induced Th1 responses to accumulate within the skin.

Keratinocyte-Intrinsic MHCII Expression Controls the Accumulation of Commensal-Induced Th1 Cells. We next sought to assess the functional consequences of MHCII expression by keratinocytes in mediating host–microbiota interactions. Strikingly, in *Il22*$^{-/-}$ mice, both MHCII expression by keratinocytes (Fig. 3 *C* and *D*) and Th1 cell accumulation was impaired following *S. epidermidis* association (Fig. 5 *A* and *B*). Furthermore, in WT mice treated with IL-22–neutralizing antibody, Th1 accumulation was also decreased (*SI Appendix*, Fig. S5*A*).
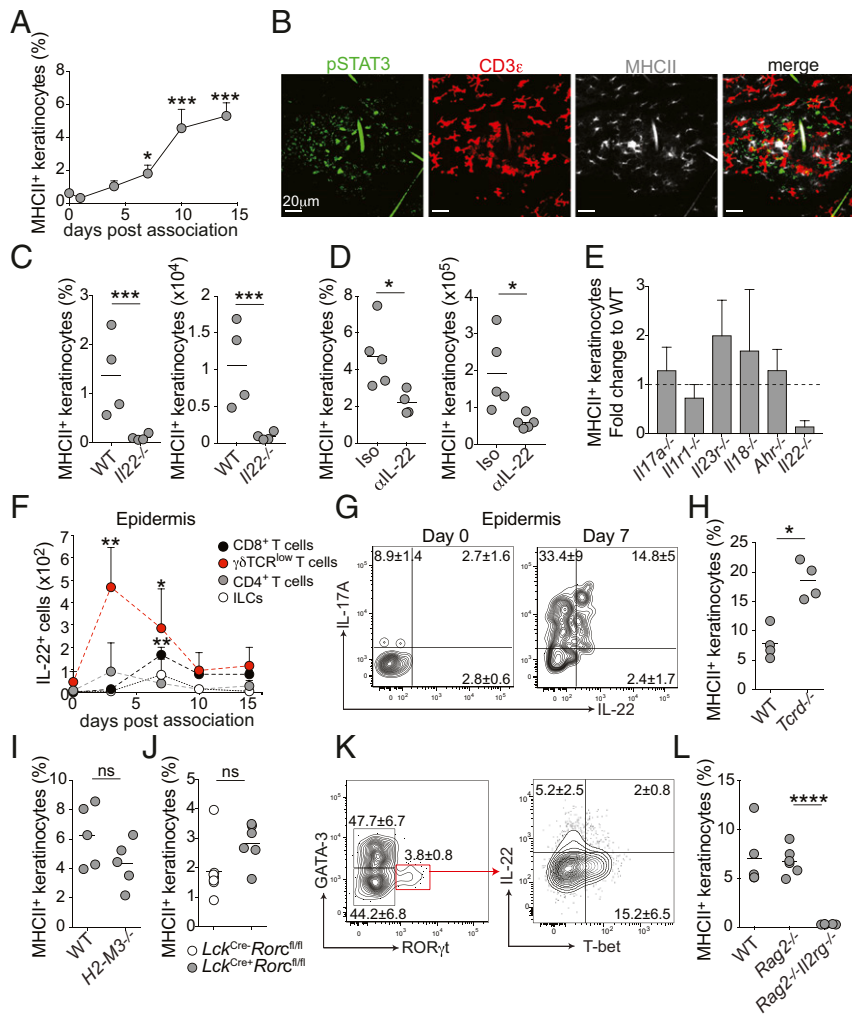
Fig. 3. IL-22 controls keratinocyte expression of MHCII. (*A*) Flow cytometric analysis of the frequency of MHCII⁺ keratinocytes at days 0, 3, 7, 10, and 14 postassociation with *S. epidermidis*. Statistics are relative to baseline at day 0 (preassociation). (*B*) Representative confocal microscopy images of a projection on the z axis of C57BL/6 mouse epidermis stained for pSTAT3, CD3ε, and MHCII at day 5 postassociation with *S. epidermidis.* (Scale bars, 20 μm.) (*C* and *D*) Frequencies and absolute numbers of CD49f⁺Sca-1⁺MHC-II⁺ keratinocytes at day 14 postassociation with *S. epidermidis* in WT and *Il22⁻/⁻* mice (*C*) and in mice treated with anti–IL-22 (αIL-22) neutralizing or isotype (Iso) control antibodies (*D*). (*E*) Fold increase in absolute number of MHCII⁺ keratinocytes in *Il17a⁻/⁻*, *Il1r1⁻/⁻*, *Il23r⁻/⁻*, *Il18⁻/⁻*, *Ahr⁻/⁻*, and *Il22⁻/⁻* mice as compared to WT control mice at day 14 postassociation with *S. epidermidis*. (*F*) Cell numbers of IL-22–producing CD4⁺ T cells, γδTCR^low cells, CD8⁺ T cells and ILCs in the epidermis at days 0, 3, 7, 10, and 14 postassociation with *S. epidermidis*. Statistics are relative to baseline at day 0 (preassociation). (*G*) Flow cytometric analysis of epidermal γδTCR^low cell for their expression of IL-17A and IL-22 at days 0 and 7 postassociation with *S. epidermidis*. (*H–J*) Frequencies of epidermal MHCII⁺ keratinocytes in *Tcrd⁻/⁻* (*H*), *H2-M3⁻/⁻* (*I*), and *Lck^creRorc^fl/fl* (*J*) mice at day 14 postassociation with *S. epidermidis*. (*K*) Flow cytometric analysis of ILCs for their expression of GATA-3, RORγt, T-bet, and IL-22 at day 7 postassociation with *S. epidermidis*. (*L*) Frequencies of MHCII⁺ keratinocytes at day 14 postassociation with *S. epidermidis* in WT, *Rag2⁻/⁻*, and *Rag2⁻/⁻Il2rg⁻/⁻* mice. Student's *t* test was used to measure significance. Data are presented as mean only or mean ± SEM. ns: nonsignificant; *$P < 0.05$, **$P < 0.01$, ***$P < 0.001$, and ****$P < 0.0001$. Data are representative of 2 to 4 independent experiments.

Of note, little is known about the factors controlling the accumulation of IFN-γ–producing T cells under noninflammatory settings. We have previously shown that following *S. epidermidis* association, Th1 cells accumulating within the skin (*SI Appendix,* Fig. S1*A*) are enriched in *S. epidermidis*-specific cells (9). Generation of bone marrow (BM) chimeric mice, (WT BM to WT recipient, and WT BM to MHCII-deficient [*Ab1⁻/⁻*] recipients) demonstrated decreased numbers of IFN-γ⁺CD4⁺ T cells in WT BM to *Ab1⁻/⁻* chimeras following *S. epidermidis* association, supporting the idea that radioresistant cells expressing MHCII were necessary for the maintenance of Th1 responses to defined microbiota members (*SI Appendix,* Fig. S5*B*). Although LCs have been shown to be radioresistant (42), mice deficient in LCs (43), developed Th1 responses and MHCII expression by keratinocytes in response to *S. epidermidis* in a manner comparable to WT mice (*SI Appendix,* Fig. S5*C*). This suggested a potential link between MHCII expression by keratinocytes and the maintenance and accumulation of Th1 responses to the microbiota.

We next assessed the possibility that Th1 accumulation within commensal-induced clusters may be associated with keratinocyte antigen presentation. However, the low biomass of skin microbes (44) precluded direct evaluation of antigen presentation of commensal-derived antigens by keratinocytes in vivo, and in vitro exposure to microbes cannot reproduce the physiological conditions associated with host–microbiota interactions. To circumvent this issue, we assessed the ability of CD49f⁺Sca-1⁺MHCII⁺ keratinocytes to uptake and process antigen using a tractable system. DQ-ovalbumen (OVA) does not fluoresce until it is proteolytically cleaved into fragments, which has been shown to correlate well with antigen processing. Ex vivo, CD49f⁺Sca-1⁺MHCII⁺ keratinocytes
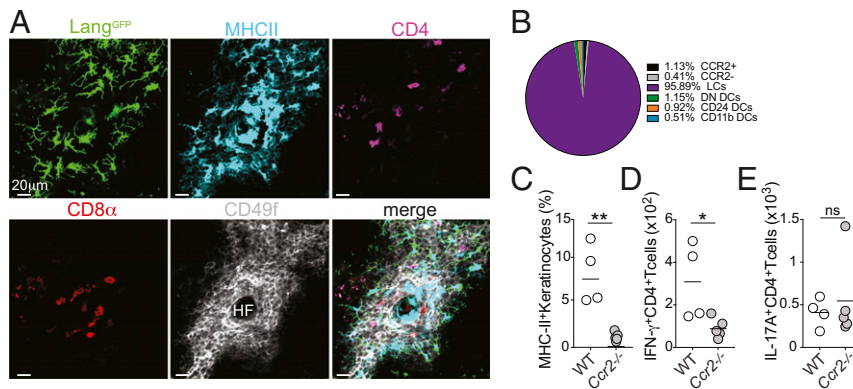
Fig. 4. MHCII+ expression on keratinocytes depends on CCR2+ monocytes and monocyte-derived cells. (*A*) Representative image of a projection on the *z* axis of epidermal skin from Langerin^GFP mouse (Lang^GFP) stained for MHCII, CD4, CD8α, and CD49f at day 14 postassociation with *S. epidermidis*. (Scale bars, 20 μm.) (*B*) Pie chart showing percentages of LCs, CCR2+ monocyte-derived cells and macrophages, CD11b+DCs, CD24+DCs, and double negative (DN) DCs in the epidermis day 14 postassociation with *S. epidermidis*. Percentages are calculated based on the total number of the cell subsets plotted on the pie chart. (*C*–*E*) Frequencies of MHCII+ keratinocytes (*C*) or absolute numbers of IFN-γ+CD4+ T cells (*D*) or IL-17A+CD4+ T cells (*E*) in WT or *Ccr2*^−/− mice at day 14 postassociation with *S. epidermidis*. Student's test was used to measure significance. Data are presented as a mean. ns, nonsignificant; *P < 0.05, **P < 0.01.

were able to uptake and process DQ-OVA protein at higher rates than CD49f+Sca-1+MHCII− keratinocytes isolated from *S. epidermidis*-associated mice (*SI Appendix*, Fig. S5D). This supports the idea that, in vivo, keratinocytes may be able to capture microbiota-derived products directly (e.g., bacteria-derived extracellular membrane vesicles within hair follicles) or indirectly (e.g., via antigen-presenting cells). Together with the increased expression of genes associated with antigen presentation and processing (Fig. 2 *F* and *G*), these data supported the idea that keratinocytes may be able to process and present commensal-derived antigens within epidermal clusters, thereby promoting the local function of commensal-induced Th1 cells. However, we cannot exclude the possibility that the role for MHCII expression on keratinocytes may not be associated with antigen presentation. Indeed, MHCII molecules can bind to several ligands, a

phenomenon that may control local T cell responses independently of cognate antigen recognition.

To directly assess a role for MHCII in keratinocyte function, we generated mice in which MHCII was conditionally deleted in keratinocytes (*Krt14*^Cre+*Ab1*^fl/fl). The skin contains several subsets of dendritic cells (45). No differences were observed in dendritic cell (DC) number and frequencies, nor in their MHCII expression between *Krt14*^Cre+*Ab1*^fl/fl and *Krt14*^Cre−*Ab1*^fl/fl control mice (*SI Appendix*, Figs. S5 *E*–*G*). To prevent any defects in the development of CD4+ T cells (46), *Krt14*^Cre+*Ab1*^fl/fl and *Krt14*^Cre−*Ab1*^fl/fl mice were surgically grafted at 3 weeks of age with a WT thymus. Notably, we found that in the absence of MHCII expression by keratinocytes in *Krt14*^Cre+*Ab1*^fl/fl mice, IFN-γ+CD4+ T cell frequencies and numbers were dramatically reduced in response to *S. epidermidis* as compared to control mice (Fig. 5 *C* and *D*). On the
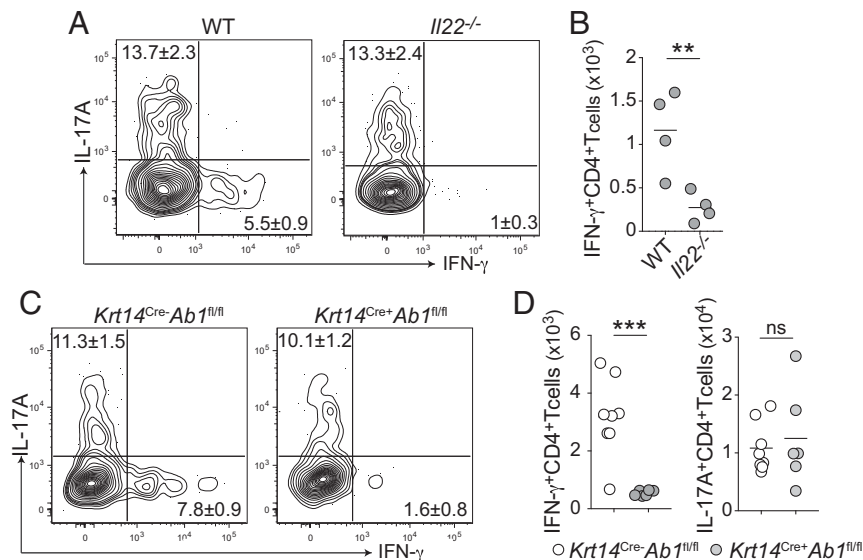
Fig. 5. MHCII+ keratinocytes sustain production of IFN-γ by CD4+ T cells. (*A*) Flow cytometric analysis of the frequency of CD4+ T cells producing IL-17A and IFN-γ in WT and *Il22*^−/− mice at day 14 postassociation with *S. epidermidis*. (*B*) Absolute numbers of IFN-γ+CD4+ T cells in WT and *Il22*^−/− mice. (*C*) Flow cytometric analysis of the frequency of CD4+ T cells producing IL-17A and IFN-γ in *Krt14*^cre+*Ab1*^fl/fl and *Krt14*^cre−*Ab1*^fl/fl mice at day 14 postassociation with *S. epidermidis*. (*D*) Absolute cell numbers of IFN-γ+CD4+ T cells and IL-17A+CD4+ T cells in *Krt14*^cre+*Ab1*^fl/fl and *Krt14*^cre−*Ab1*^fl/fl mice at day 14 postassociation with *S. epidermidis*. Student's *t* test was used to measure significance. Data are presented as mean only or mean ± SEM. ns: nonsignificant, **P < 0.01 and ***P < 0.001. Data are representative of 2 to 4 independent experiments.

IMMUNOLOGY AND INFLAMMATION

other hand, the production of IL-17A by CD4$^+$ T cells remained unchanged, further supporting the idea that an IL-22/keratinocyte MHCII axis plays a defined role in the control immune responses to commensals.

Discussion

While all body surfaces are constantly exposed to new microbes, the rules governing the tonic recognition of these commensals remain poorly understood. Here we show that keratinocytes play an unexpected role in the control of the quality of commensal-induced T cells. While epithelial cells can express MHCII both under homeostasis and in the context of inflammation (27, 47, 48), the functional consequences of MHCII expression by non-conventional antigen-presenting cells remains poorly understood. In vitro, activated keratinocytes have been shown to be able to present antigen (49). Several reports also support the idea that, under defined inflammatory or infectious experimental settings, keratinocytes can function as antigen-presenting cells for local reactivation of lymphocytes (50–52). Recent work also revealed a surprising expression of MHCII by a subset of intestinal stem cells, a phenomenon shown to impact epithelial cell differentiation and fate during infection (47). Here we show that under steady-state conditions, MHCII expression by keratinocytes plays an important role in mediating the host–microbiota dialogue.

Our results support the idea that this process is coordinated by IL-22. While a role for this cytokine in the promotion of skin inflammation is now well established (33), less is understood about the physiological role of IL-22 within the skin under noninflammatory settings. In our present study, the IL-22/MHCII axis was independent of classic factors known to induce IL-22, such as IL-23, IL-1, or Ahr signaling, further supporting the idea that the factors involved in the homeostatic control of commensal-induced T cells are highly distinct from those in place to co-ordinate inflammatory responses. In our setting, whether the role of MHCII on keratinocytes relies on true antigen presentation versus ligand binding remains unclear. Indeed, MHCII can bind to several ligands such as LAG-3 (53), a phenomenon that may control local T cell responses independently of cognate antigen recognition. On the other hand, if antigens contribute to the local reactivation of commensal-induced Th1 cells, how commensal-derived antigens are sensed and acquired by keratinocytes remains to be addressed. Nonetheless, in support of a role for antigen-presenting cell function, MHCII-expressing keratinocytes also up-regulated the expression of numerous genes associated with antigen processing and presentation.

The microbiota has been shown to promote tissue accumulation of both type 1 and type 17 cells (4, 7, 54–56). While the factors controlling commensal-induced Th17 or Tc17 stability and accumulation have been well explored both in the gut and the skin (4, 5, 7, 9, 57), little is known about the factors controlling commensal-induced Th1 cells. Within the gut compartment, accumulation of inflammatory Th1 cells in response to a member of the microbiota has been shown to depend on IL-18 (54, 58), a factor that we found dispensable for the homeostatic accumulation of Th1 cells in response to a commensal within the skin.

Our observation that MHCII$^+$ keratinocytes exclusively control commensal-induced Th1, but not Th17 cells, is intriguing. Such dichotomy may reflect a differential requirement for local costimulation and chemokines produced by activated keratinocytes. Indeed, in addition to genes associated with antigen processing and presentation, cluster-associated keratinocytes expressed chemokines known to promote T cell accumulation and function, including *Ccl20* and *Cxcl9/10* (24, 25). Furthermore, MHCII$^+$ keratinocytes expressed a large number of genes associated with antimicrobial defense, supporting the idea that commensal-induced clusters may play an important role in tissue immune surveillance.

Altogether, our work uncovers an unexpected role for MHCII$^+$ keratinocytes in the local licensing of commensal-induced T cells, findings that provide an understanding of the tissue-specific rules governing host–microbiota interactions.

Experimental Procedures

Animals. C57BL/6NTac (B6) specific pathogen-free mice were purchased from Taconic Farms. Germ-free C57BL/6 mice were bred and maintained in the National Institute of Allergy and Infectious Diseases (NIAID) Microbiome Program gnotobiotic animal facility. CD45.1 B6 [B6.SJL-Cd45a(Ly5a)/Nai], B10.A [B10.A-Cd45a(Ly5a)/NAi N5], T-bet^{ZsGreen} (C57BL/6-Tbet-ZsGreen [Tg]), *Il1r1$^{-/-}$* (C57BL/6-[KO]IL1r1), *Rag1$^{-/-}$* (B6.129S7-Rag1^{tm1Mom}), *Rag2$^{-/-}$* (C57BL/10SgSnAi-[KO]RAG2), *Rag2$^{-/-}$Il2rg$^{-/-}$* (B10.SJL-Cd45a(Ly5a)-[KO]RAG2-[KO]γc), *Il17a$^{-/-}$* (C57BL/6-[KO]IL17A), *Ifng$^{-/-}$* (C57BL/6Tac-[KO]IFN γ N12), *Tnfa$^{-/-}$* (C57BL/6J-[KO]TNF-α), *Ifnar$^{-/-}$* (B6-[KO]IFNa/b R1), *Ab1$^{-/-}$* (C57BL/6NTac-[KO]Abβ N22) mice were obtained through the NIAID-Taconic exchange program. R26-stop-EYFP [B6.129 × 1-Gt(ROSA)$^{26Sortm1(EYFP)Cos}$/J], *Ab1$^{fl/fl}$* (B6.129 × 1-H2-Ab1^{tm1Koni}/J), *Krt14^{Cre}* [B6N.Cg-Tg(KRT14-cre)^{1Amc}/J], *Ahr$^{-/-}$* (B6.129-Ahr^{tm1Bra}/J), and *Tcrd$^{-/-}$* (B6.129P2-Tcrd^{tm1Mom}/J) mice were purchased from the Jackson Laboratory. *Il17a^{Cre}* mice were kindly provided by B. Stockinger, The Francis Crick Institute, London, United Kingdom. *H2-M3$^{-/-}$* mice were kindly provided by C. Wang, Northwestern University, Evanston, IL, and bred in house with WT C57BL/6. *Il23r$^{-/-}$* and *Il22^{RFP}* mice were a kind gift from M. Oukka, Seattle Children's Research Institute, Seattle, WA. *Il18$^{-/-}$* (B6.129P2-Il18^{tmAki}/J) mice were obtained from G. Trinchieri National Cancer Institute (NCI)/NIH, Bethesda, MD. *Il22$^{-/-}$* mice were obtained from Pfizer. *Il22-tdTomato* mice were provided by S. K. Durum (NCI/NIH). B6.FVB-Tg(CD207-Dta)312Dhka/J (Lang^{DTA}) were kindly provided by D. Kaplan, University of Minnesota, Minneapolis, MN. *Lck^{Cre} Rorc$^{fl/fl}$* mice were kindly provided by R. N. Germain NIAID/NIH, Bethesda, MD. All mice were bred and maintained under pathogen-free conditions at an American Association for the Accreditation of Laboratory Animal Care-accredited animal facility at the NIAID and housed in accordance with the procedures outlined in the *Guide for the Care and Use of Laboratory Animals* (59). All experiments were performed at the NIAID under an animal study proposal (LISB-20E) approved by the NIAID Animal Care and Use Committee. Sex- and age-matched mice between 6 and 12 weeks of age were used for each experiment. Wild mice (*Mus musculus domesticus*) were trapped in Maryland and the District of Columbia and housed as previously described (19), with the approval of the relevant regulatory bodies under a protocol approved by the National Institute of Diabetes and Digestive and Kidney Diseases (NIDDK) Animal Care and Use Committee. For mice reconstituted with wild-mouse microbiota, embryos of C57BL/6 mice were generated in vivo at the NIDDK animal facility, isolated, and transferred in pseudopregnant wild females. Those litters were used to establish a colony of C57BL/6 mice with wild-mouse microbiota and the colony was handled under BSL2 conditions with BSL3 practices, as previously described (20).

Topical Association of Mice with Commensal Isolates. *S. epidermidis* strains (NIHLM061, NIH05001, and NIHLM087) and *S. aureus* (42F02) were cultured for 18 h in Tryptic Soy Broth at 37 °C without shaking. *C. albicans* was cultured for 18 h in Tryptic Soy Broth at 30 °C with shaking (180 rpm). For topical association of bacteria or fungi, each mouse was associated with a bacterial or fungal suspension (~10^9 colony-forming unit [CFU]/mL) across the surface of the ear pinnae or across the entire back skin using a sterile cotton swab. Topical application was repeated 4 times every other day before analysis. For topical application of various bacterial species or strains, 18-h cultures were normalized at OD$_{600}$ to obtain similar bacterial density (~10^9 CFU/mL).

BM Chimera. WT B6 (CD45.2) or *Ab1$^{-/-}$* (CD45.2) mice were lethally irradiated with 2 doses of 525 Rads, 5 h apart, and then injected intravenously with 1.5 × 10^6 BM cells from femurs and tibias of WT CD45.1 mice. Irradiated and reconstituted mice were given Bactrim (sulfamethoxazole [150 mg/mL] and *N*-trimethoprim [30 mg/mL]) in their drinking water for 2 weeks and switched thereafter to sterile drinking water. Mice were allowed to reconstitute for 6 to 8 weeks before topical association with *S. epidermidis*.

Murine Tissue Processing. Cells from ear pinnae and back skin were isolated as previously described (3). Ear pinnae and back tissues were digested in digestion media (RPMI 1640 media supplemented with 2 mM L-glutamine, 1 mM sodium pyruvate and nonessential amino acids, 55 μM β-mercaptoethanol, 20 mM Hepes, 100 U/mL penicillin, 100 μg/mL streptomycin and 0.25 mg/mL Liberase TL [Roche]), and incubated for 1.5 h at 37 °C and 5% CO$_2$. Digested

skin sheets were grinded using the Medicon/Medimachine tissue homogenizer system (Becton Dickinson). To separate epidermis from dermis, ear pinnae was first digested for 45 min with 500 CU Dispase (Becton Dickinson) in HBSS without calcium and magnesium. Epidermis was then peeled from dermis with curved forceps, washed in PBS and successively cut with scissors, digested with Liberase TL digestion media for 1.5 h at 37 °C and 5% CO_2, homogenized by pipetting up and down, and finally filtered through 70-μm cell strainer.

Immunofluorescence/Confocal Microscopy of Ear Pinnae. Ear pinnae were split with forceps, fixed in 1% paraformaldehyde solution (Electron Microscopy Sciences) overnight at 4 °C, and blocked in 1% BSA, 0.25% Triton X blocking buffer for 2 h at room temperature. Tissues were stained with anti-CD8α (clone 53-6.7, Life Technologies eBioscience), anti-CD49f (eBioGoH3, Life Technologies eBioscience), anti-MHCII (M5/114.15.2, Life Technologies eBioscience), anti-CD4 (RM4-5, Life Technologies eBioscience), and/or rabbit anti-GFP Alexa Fluor 488 (Life Technologies Invitrogen) antibodies overnight at 4 °C, and washed 3 times with PBS before being mounted with ProLong Gold (Molecular Probes) antifade reagent. For pSTAT3 staining, tissues were fixed in 10% formalin in PBS for 1 h and then stained with anti-CD3ε (145-2C11, Life Technologies eBioscience), anti-MHCII (M5/114, Life Technologies eBioscience), and anti-pSTAT3 (D3A7, Cell Signaling Technology) in 1% BSA, 0.25% Triton X blocking buffer. Tissues were then washed 3 times in blocking buffer and then stained with goat anti-Rabbit IgG (H+L) Alexa Fluor 488 (Life technologies) for 6 h. Ear pinnae images were captured on a Leica TCS SP8 confocal microscope with a 40× oil objective (HC PL APO 40×/1.3 oil). Images were analyzed using Imaris Bitplane software.

Phenotypic Analysis. Single-cell suspensions were incubated with fluorochrome-conjugated antibodies against surface markers, as previously described (3): CD4 (clone RM4-5), CD8β (eBioH35-17.2), CD11b (M1/70), CD11c (N418), CD19 (6D5), CD24 (M1/69), CD45 (30-F11), CD45.1 (A20), CD45.2 (104), CD64 (X54-5/7.1), Ly-6C (HK1.4), Ly-6G (1A8), MHCII (M5/114.15.2), TCRβ (H57-597), CD45R (RA3-6B2), CD49f (eBioGoH3), CD90.2 (53–2.1), CD31 (MEC13.3), CD34 (RAM34), Sca-1 (D7), Siglec-F (E50-2440), and EpCAM (G8.8) in PBS for 30 min at 4 °C and then washed. LIVE/DEAD Fixable Blue Dead Cell Stain Kit (Life Technologies Invitrogen) was used to exclude dead cells. Cells were then fixed for 20 min at 4 °C using BD Cytofix/Cytoperm (Becton Dickinson) and washed twice. For intracellular cytokine staining, cells were stained with fluorochrome-conjugated antibodies against IFN-γ (XMG-1.2), IL-17A (eBio17B7), IL-22 (IL22JOP), and Foxp3 (FJK-16s) using Foxp3/Transcription Factor staining buffer set (Life Technologies eBioscience) for 2 h at 4 °C. For detection of cytokine potential, single-cell suspensions from various tissues were cultured directly ex vivo, as previously described (3). After stimulation, cells were assessed for surface markers and intracellular cytokine production as described below. For transcription factor staining and cytokine staining (3), cells were fixed and permeabilized with the Foxp3/Transcription Factor staining buffer set (Life Technologies eBioscience) and stained with fluorochrome-conjugated antibodies against GATA-3 (L50-823 or TWAJ), T-bet (eBio4B10), or RORγt (B2D) for 2 h at 4 °C. Each staining was performed in the presence of purified anti-mouse CD16/32 (2.4G2), 0.2 mg/mL purified rat γ-globulin (Jackson Immunoresearch). All antibodies were purchased from Life Technologies eBioscience, Biolegend or BD Biosciences. Cell acquisition was performed on a BD Fortessa X-20 flow cytometer using FACSDiVa software (BD Biosciences) and analyzed using FlowJo software (TreeStar).

DQ-OVA Assay. Approximately 2,000 cells isolated from a cell suspension of ear pinnae were incubated at 37 °C, 5% CO_2 for 45 min in 200 uL of RPMI 10% FBS with or without DQ-OVA (50 ug/mL, D12053, Invitrogen). Cells were then washed and stained for direct flow-cytometric analysis of keratinocytes and DCs, as described above.

In Vivo Antibody Administration. Mice were treated intraperitoneally with 0.1 mg of anti–IL-22 neutralizing antibody (clone 8E11) or isotype control antibody, daily starting 3 d prior association with *S. epidermidis* NIHLM087.

In Vivo Proliferation of Keratinocytes. Proliferation of keratinocytes was assessed using the Click-iT EdU Alexa Fluor 647 Flow Cytometric Assay Kit (Invitrogen C10419). Mice were injected with 1 mg of EdU intraperitoneally 16 h before analysis, and ear pinnae were processed and analyzed by flow cytometry following the manufacturer's recommendation.

Keratinocyte Isolation and RNA Extraction for RNA-Seq. Keratinocytes were FACS-sorted from ear pinnae epidermis of C57BL/6 mice from unassociated mice or day 14 posttopical association with *S. epidermidis* NIHLM087. CD49f$^+$Sca-1$^+$ keratinocytes were sorted as CD45$^-$CD31$^-$CD34$^-$ cells and further separated based on their expression of MHCII. RNA was extracted from 60,000 keratinocytes per replicate using the RNAeasy micro Kit for RNA Isolation (Qiagen), as per the manufacturer's instructions.

RNA Library Preparation and Sequencing. mRNA libraries were constructed using the SMARTer Ultra Low Input RNA kit (Clontech) followed by the Nextera XT DNA library prep kit (Illumina). Samples were sequenced paired-end for 79 bp on an Illumina NextSeq500 machine. Sequencing quality was assessed using FASTQC v0.11.5 and aligned to the mm10 reference genome using bowtie2 (60) with RSEM (61). Differential gene expression was assessed using DESeq2 (62) with a fold-change cutoff of 2, false-discovery rate < 0.05. Functional annotation for differentially expressed genes was done with IPA (Qiagen). For comparison of control and *S. epidermidis*-associated MHCII$^-$ and MHCII$^+$ keratinocytes to different subsets of keratinocytes, lists of signature genes (versus baseline) from published single-cell RNA-seq data were downloaded (21) and overlaid with gene expression (normalized to transcripts per million) from the 3 different datasets. Relative expression was calculated for all genes with a transcript per million gene expression of at least 16.

Statistical Analysis. Groups were compared with Prism software (GraphPad) using the 2-tailed unpaired Student's *t* test. Flow cytometry plots are presented as mean ± SEM. All other data are presented as mean only or mean ± SEM. $P < 0.05$ was considered significant unless otherwise stated. Significance of clustering by PCA was tested using the PERMANOVA test as implemented in the 'adonis' R package.

1. Y. Belkaid, O. J. Harrison, Homeostatic immunity and the microbiota. *Immunity* **46**, 562–576 (2017).
2. K. Honda, D. R. Littman, The microbiota in adaptive immune homeostasis and disease. *Nature* **535**, 75–84 (2016).
3. J. L. Linehan et al., Non-classical immunity controls microbiota impact on skin immunity and tissue repair. *Cell* **172**, 784–796.e18 (2018).
4. O. J. Harrison et al., Commensal-specific T cell plasticity promotes rapid tissue adaptation to injury. *Science* **363**, eaat6280 (2019).
5. T. Sano et al., An IL-23R/IL-22 circuit regulates epithelial serum amyloid A to promote local effector Th17 responses. *Cell* **163**, 381–393 (2015).
6. C. A. Thaiss, N. Zmora, M. Levy, E. Elinav, The microbiome and innate immunity. *Nature* **535**, 65–74 (2016).
7. S. Naik et al., Compartmentalized control of skin immunity by resident commensals. *Science* **337**, 1115–1119 (2012).
8. V. K. Ridaura et al., Contextual control of skin immunity and inflammation by *Corynebacterium*. *J. Exp. Med.* **215**, 785–799 (2018).
9. S. Naik et al., Commensal-dendritic-cell interaction specifies a unique protective skin immune signature. *Nature* **520**, 104–108 (2015).
10. S. N. Mueller, L. K. Mackay, Tissue-resident memory T cells: Local specialists in immune defence. *Nat. Rev. Immunol.* **16**, 79–89 (2016).
11. Y. Natsuaki et al., Perivascular leukocyte clusters are essential for efficient activation of effector T cells in the skin. *Nat. Immunol.* **15**, 1064–1069 (2014).
12. N. Collins et al., Skin CD4(+) memory T cells exhibit combined cluster-mediated retention and equilibration with the circulation. *Nat. Commun.* **7**, 11514 (2016).

13. N. Iijima, A. Iwasaki, T cell memory. A local macrophage chemokine network sustains protective tissue-resident memory CD4 T cells. *Science* **346**, 93–98 (2014).
14. K. Nagao *et al.*, Stress-induced production of chemokines by hair follicles regulates the trafficking of dendritic cells in skin. *Nat. Immunol.* **13**, 744–752 (2012).
15. E. Fuchs, Scratching the surface of skin development. *Nature* **445**, 834–842 (2007).
16. J. Agudo *et al.*, Quiescent tissue stem cells evade immune surveillance. *Immunity* **48**, 271–285.e5 (2018).
17. M. M. Carr, E. McVittie, K. Guy, D. J. Gawkrodger, J. A. Hunter, MHC class II antigen expression in normal human epidermis. *Immunology* **59**, 223–227 (1986).
18. L. K. Beura *et al.*, Normalizing the environment recapitulates adult human immune traits in laboratory mice. *Nature* **532**, 512–516 (2016).
19. S. P. Rosshart *et al.*, Wild mouse gut microbiota promotes host fitness and improves disease resistance. *Cell* **171**, 1015–1028.e13 (2017).
20. S. P. Rosshart *et al.*, Laboratory mice born to wild mice have natural microbiota and model human immune responses. *Science* **365**, eaaw4361 (2019).
21. S. Joost *et al.*, Single-cell transcriptomics reveals that differentiation and spatial signatures shape epidermal and hair follicle heterogeneity. *Cell Syst* **3**, 221–237.e9 (2016).
22. J. Schauber, R. L. Gallo, Expanding the roles of antimicrobial peptides in skin: Alarming and arming keratinocytes. *J. Invest. Dermatol.* **127**, 510–512 (2007).
23. N. Satoh-Takayama *et al.*, The chemokine receptor CXCR6 controls the functional topography of interleukin-22 producing intestinal innate lymphoid cells. *Immunity* **41**, 776–788 (2014).
24. E. G. Harper *et al.*, Th17 cytokines stimulate CCL20 expression in keratinocytes in vitro and in vivo: Implications for psoriasis pathogenesis. *J. Invest. Dermatol.* **129**, 2175–2183 (2009).
25. A. Zaid *et al.*, Chemokine receptor-dependent control of skin tissue-resident memory T cell formation. *J. Immunol.* **199**, 2451–2459 (2017).
26. C. Dietrich, Antioxidant functions of the aryl hydrocarbon receptor. *Stem Cells Int.* **2016**, 7943495 (2016).
27. J. E. Wosen, D. Mukhopadhyay, C. Macaubas, E. D. Mellins, Epithelial MHC class II expression and its role in antigen presentation in the gastrointestinal and respiratory tracts. *Front. Immunol.* **9**, 2144 (2018).
28. P. Hruz, S. M. Dann, L. Eckmann, STAT3 and its activators in intestinal defense and mucosal homeostasis. *Curr. Opin. Gastroenterol.* **26**, 109–115 (2010).
29. S. Sano, K. S. Chan, J. DiGiovanni, Impact of Stat3 activation upon skin biology: A dichotomy of its role between homeostasis and diseases. *J. Dermatol. Sci.* **50**, 1–14 (2008).
30. G. Pickert *et al.*, STAT3 links IL-22 signaling in intestinal epithelial cells to mucosal wound healing. *J. Exp. Med.* **206**, 1465–1472 (2009).
31. K. Mao *et al.*, Innate and adaptive lymphocytes sequentially shape the gut microbiota and lipid metabolism. *Nature* **554**, 255–259 (2018).
32. R. Sabat, W. Ouyang, K. Wolk, Therapeutic opportunities of the IL-22-IL-22R1 system. *Nat. Rev. Drug Discov.* **13**, 21–38 (2014).
33. J. A. Dudakov, A. M. Hanash, M. R. van den Brink, Interleukin-22: Immunobiology and pathology. *Annu. Rev. Immunol.* **33**, 747–785 (2015).
34. B. Roediger *et al.*, Cutaneous immunosurveillance and regulation of inflammation by group 2 innate lymphoid cells. *Nat. Immunol.* **14**, 564–573 (2013).
35. B. S. Kim *et al.*, TSLP elicits IL-33-independent innate lymphoid cell responses to promote skin inflammation. *Sci. Transl. Med.* **5**, 170ra16 (2013).
36. E. Vivier *et al.*, Innate lymphoid cells: 10 years on. *Cell* **174**, 1054–1066 (2018).
37. C. Luci *et al.*, Influence of the transcription factor RORgammat on the development of NKp46+ cell populations in gut and skin. *Nat. Immunol.* **10**, 75–82 (2009).
38. S. L. Sanos *et al.*, RORgammat and commensal microflora are required for the differentiation of mucosal interleukin 22-producing NKp46+ cells. *Nat. Immunol.* **10**, 83–91 (2009).
39. L. C. Rankin *et al.*, Complementarity and redundancy of IL-22-producing innate lymphoid cells. *Nat. Immunol.* **17**, 179–186 (2016).
40. R. G. Klein Wolterink *et al.*, Pulmonary innate lymphoid cells are major producers of IL-5 and IL-13 in murine models of allergic asthma. *Eur. J. Immunol.* **42**, 1106–1116 (2012).
41. N. V. Serbina, E. G. Pamer, Monocyte emigration from bone marrow during bacterial infection requires signals mediated by chemokine receptor CCR2. *Nat. Immunol.* **7**, 311–317 (2006).
42. M. Merad *et al.*, Langerhans cells renew in the skin throughout life under steady-state conditions. *Nat. Immunol.* **3**, 1135–1141 (2002).
43. B. Z. Igyártó *et al.*, Skin-resident murine dendritic cell subsets promote distinct and opposing antigen-specific T helper cell responses. *Immunity* **35**, 260–272 (2011).
44. Y. Belkaid, J. A. Segre, Dialogue between skin microbiota and immunity. *Science* **346**, 954–959 (2014).
45. S. Tamoutounour *et al.*, Origins and functional specialization of macrophages and of conventional and monocyte-derived dendritic cells in mouse skin. *Immunity* **39**, 925–938 (2013).
46. Y. M. Morillon, 2nd, F. Manzoor, B. Wang, R. Tisch, Isolation and transplantation of different aged murine thymic grafts. *J. Vis. Exp.* **99**, e52709 (2015).
47. M. Biton *et al.*, T helper cell cytokines modulate intestinal stem cell renewal and differentiation. *Cell* **175**, 1307–1320.e22 (2018).
48. C. P. Stringer, R. Hicks, P. A. Botham, The expression of MHC class II (Ia) antigens on mouse keratinocytes following epicutaneous application of contact sensitizers and irritants. *Br. J. Dermatol.* **125**, 521–528 (1991).
49. A. P. Black *et al.*, Human keratinocyte induction of rapid effector function in antigen-specific memory CD4+ and CD8+ T cells. *Eur. J. Immunol.* **37**, 1485–1493 (2007).
50. B. S. Kim *et al.*, Keratinocytes function as accessory cells for presentation of endogenous antigen expressed in the epidermis. *J. Invest. Dermatol.* **129**, 2805–2817 (2009).
51. B. L. Macleod *et al.*, Distinct APC subtypes drive spatially segregated CD4+ and CD8+ T-cell effector activity during skin infection with HSV-1. *PLoS Pathog.* **10**, e1004303 (2014).
52. L. Fan *et al.*, Antigen presentation by keratinocytes directs autoimmune skin disease. *Proc. Natl. Acad. Sci. U.S.A.* **100**, 3386–3391 (2003).
53. L. T. Nguyen, P. S. Ohashi, Clinical blockade of PD1 and LAG3—Potential mechanisms of action. *Nat. Rev. Immunol.* **15**, 45–56 (2015).
54. K. Atarashi *et al.*, Ectopic colonization of oral bacteria in the intestine drives T_H1 cell induction and inflammation. *Science* **358**, 359–365 (2017).
55. J. A. Hall *et al.*, Commensal DNA limits regulatory T cell conversion and is a natural adjuvant of intestinal immune responses. *Immunity* **29**, 637–649 (2008).
56. V. Gaboriau-Routhiau *et al.*, The key role of segmented filamentous bacteria in the coordinated maturation of gut helper T cell responses. *Immunity* **31**, 677–689 (2009).
57. I. I. Ivanov *et al.*, Induction of intestinal Th17 cells by segmented filamentous bacteria. *Cell* **139**, 485–498 (2009).
58. A. Chudnovskiy *et al.*, Host-protozoan interactions protect from mucosal infections through activation of the inflammasome. *Cell* **167**, 444–456.e14 (2016).
59. National Research Council, *Guide for the Care and Use of Laboratory Animals* (National Academies Press, Washington, DC, ed. 8, 2011).
60. B. Langmead, S. L. Salzberg, Fast gapped-read alignment with Bowtie 2. *Nat. Methods* **9**, 357–359 (2012).
61. B. Li, C. N. Dewey, RSEM: Accurate transcript quantification from RNA-seq data with or without a reference genome. *BMC Bioinformatics* **12**, 323 (2011).
62. M. I. Love, W. Huber, S. Anders, Moderated estimation of fold change and dispersion for RNA-seq data with DESeq2. *Genome Biol.* **15**, 550 (2014).